Intercellular aspirin hand-over with dual therapies by liposome-loaded monocytes

Hak-Joon Sung (hj72sung@yuhs.ac)
Yonsei University College of Medicine https://orcid.org/0000-0003-2312-2484
Seung Eun Yu
Yonsei University College of Medicine
Jueun Kim
Yonsei University College of Medicine
Dae-Hyun Kim
Chungnam National University Daejeon
Sewoom Baek
Yonsei University College of Medicine
Suji Park
Yonsei University College of Medicine
Seyong Chung
Yonsei University College of Medicine

Article

Keywords:

Posted Date: January 12th, 2024

DOI: https://doi.org/10.21203/rs.3.rs-3815496/v1

Additional Declarations: There is **NO** Competing Interest.

Abstract

Cell-cell communication serves as a foundation concept of intercellular therapeutic hand-over. Despite the commonsense level of understanding, no clear projection has been made to prove the mechanism. Here, the hand-over of aspirin-liposomes from monocytes to inflamed cells is validated under high-resolution time series of 3D imaging in vitro with in vivo confirmation. As a significant value, caveolin is identified to play a major role in mediating the hand-over using cell receptors by super-resolution microscopy, which is induced by the overexpression of caveolin upon inflammation. When aspirin-liposomes are loaded to splenic monocytes, they naturally target inflamed sites efficiently because the spleen is a major site of liposomal clearance from the body in addition to monocyte residence to leave towards inflammatory signals. The delivery efficiency and anti-inflammatory effects of hand-over through intravenous injection are superior to oral injection of soluble aspirin as confirmed in the ischemic hindlimb and fatty liver of mice (targeted therapy). These results are also agreed by the anti-platelet effect in mouse blood over 7 days (prolonged therapy), and the combination of these therapeutic actions effectively rescues atherosclerotic carotid artery of mouse. This study proves the working mechanism of hand-over, suggesting a translational strategy to improve intercellular delivery.

Introduction

Therapeutic delivery undergoes systemic circulation to reach target cells, and the effect propagates to even untargeted cells. Continuous progress has been made in approaching the pin-point targeting from systemic injection to cells[1–4]. However, clear hand-over mechanisms remain unproven as tossing and receiving of therapeutics from targeted cells to untargeted neighbors are merely understood at the level of commonsense[5]. The paradigm of cell-cell communication simply projects a theoretical picture of hand-over mechanism. As a potential mediator of hand-over to inflamed cells, caveolin plays a major role in endocytosis of external signaling molecules[6–9], and its expression is increased in inflamed cells[6–8, 10, 11], thereby handling the inflammatory signaling and responses[8, 9, 12]. These facts rationalize the receiver role of caveolin in inflamed cells upon tossing from target cells such as monocytes. Along the same line, the recruitment of monocytes to the inflamed sites increases when the inflammation level is elevated[13, 14], indicating increases in the demand of hand-over to amplify the anti-inflammatory effects of therapeutics[6–8, 10, 11].

Nanoparticle-loading onto monocytes has been proven to target inflamed sites efficiently[13, 15, 16]. The spleen serves as a major site where therapeutic delivery is cleared from the body[17, 18], and monocytes reside to leave spontaneously towards inflammatory sites[13, 16]. Therapeutic loading to splenic monocytes provides advantages of inflammation-triggered (stimuli-responsive) targeting from the residence site[13], thereby avoiding systemic side effects of therapeutics. In this way, the therapeutic effect can be focused on the inflamed site by reducing the therapeutic dose. As another advantage of this approach, the therapeutic effect on blood can be prolonged under circulation as most nanoparticles are known to be

cleared from the circulation within 2 ~ 3 days[13,14], but a large portion of them is captured by circulating or splenic monocytes whose blood circulation is even inevitable for actions[13,14].

Aspirin has been used more than a century with worldwide consumption of hundred billion pills in a year[19] due to the anti-inflammatory and anti-thrombotic effects[20–23]. As a challenging point of use, aspirin usually degrades in hepatocytes with a half-life of 2 h[24] so the daily intake is mandatory. In this regard, although aspirin delivery to inflamed endothelial cells (ECs) has been shown to exert anti-inflammatory effects by repairing endothelial dysfunctions[20–23], the delivery method has not been established to reach clinical translation. Increasing the aspirin dose to treat vascular atherosclerosis results in no improvement of therapeutic outcomes according to a recent clinical report from randomized trials with over 15,000 patients[25]. This report indicates an unmet need to control the aspirin dose to focus the effect on a target. The aspirin treatment for vascular atherosclerosis has been approached by mainly considering the anti-platelet effect[20–23]. Hence, the combination with the anti-inflammatory therapy can be proposed to open another avenue by repositioning the world-class drug for the aging population.

This study applies these rationales and thereby validates the working mechanism of hand-over from splenic monocytes to inflamed cells and platelets upon targeting and under prolonged circulation, respectively. Aspirin is encapsulated by liposomes, which are loaded to monocytes through tail vein injection in mice by relying on splenic docking between clearing liposomes and residing monocytes. The inflammation-responsive targeting and therapy of monocytes with aspirin-liposomes on inflamed ECs and hepatocytes are validated in ischemic hindlimb and fatty liver in mice. As a scientific value to emphasize, caveolin leads a receiver role in the hand-over into inflamed cells by co-operating with clathrin. The leading role of caveolin is mediated by the endocytic function upon over-expression under inflammation which increases the demand of hand-over by monocytes. The combination of targeted effect with the prolonged anti-platelet therapy through circulation over 7 days rescues the atherosclerotic carotid artery in mice. The monocyte carrier and caveolin receiver of liposomes exert superior therapeutic effects of aspirin compared to the oral intake of aspirin in the mouse models. Of note, advanced methods are employed including lattice light-sheet microscopy with time series 3D imaging and super-resolution microscopy with analysis of artificial intelligence (AI)-driven automated segmentation.

Results

1. Liposomal loading to monocyte for hand-over to inflamed cells

As an overarching hypothesis, the liposomal loading to monocytes leads to subsequent hand-over to inflamed cells upon inherent targeting, and this process is dominantly mediated by caveolin because of the expressional upregulation under inflammation. This strategy enables the dual therapies of aspirin by reducing i) not only the inflammation in target sites ii) but also platelet activation upon prolonged systemic circulation (Fig. 1a). As the first step, liposomes (+/- aspirin) are produced through rapid

injection and exhibit a circular shape under imaging by transmission electron microscopy (TEM) with around 100 nm in diameter as examined by dynamic light scattering (DLS) **(Extended data** Fig. 1a-b**)**.

When fluorescent-tagged liposomes are injected into each mouse through the tail vein, dominant distribution signals are detected in the liver and spleen in in vivo imaging system (IVIS) **(Extended data** Fig. 1c**)**. Then, cells are extracted from the spleen and separated to the CD11b-positive (monocytes) and negative groups. The $CD11b^{+}$ monocytes exhibit the strong fluorescence intensity as an indication of liposomal uptake in contrast to the poor signal in other cells **(Extended data** Fig. 1d**)**. This result is confirmed by the fluorescence-activated cell sorting (FACS) analysis with staining CD11b of monocytes as 25% of the population uptakes liposomes within a day **(Extended data** Fig. 1e**)**. As another evidence, the red (DiD) liposomes are shown up between the green CD11b of membrane and the blue nucleus inside the monocytes upon immunostaining **(Extended data** Fig. 1f**)**. The result is further confirmed under TEM imaging as gold (10 nm)-tagged liposomes are presented in a circular liposome-like shape inside the monocytes **(Extended data** Fig. 1g**)**. These results validate the liposomal loading onto monocytes via tail vein injection.

Fluorescent (DiO)-tagged liposomes are loaded into monocytes, which are then co-cultured with either ECs or hepatocytes in the top and bottom of trans-wells, respectively, as shown in the illustration **(**Fig. 1b**)**. When inflammation is induced by lipopolysaccharide (LPS) or ethanol, the inflamed ECs and hepatocytes (green phalloidin) uptake the liposome (red) significantly more compared to non-inflamed condition as indicated by co-localization of red liposomes and green cytoskeleton. The quantitative image analysis of internalized aspirin-liposome validates the inflamed cell-specific hand-over **(**Fig. 1c**)**. Also, gold (10 nm) dots are seen in lining the circles inside the inflamed EC under TEM imaging as an indication of hand-over of liposomes from monocytes to inflamed ECs **(Extended data** Fig. 2a**)**.

Next, this hand-over process is visualized under 3D high-resolution imaging by lattice light-sheet microscopy because it is possible for liposomes to attach merely on the membrane surface of inflamed cells rather than internalization **(**Fig. 1d **and Supplementary video 1)**. The imaging captures the gradual progress in liposomal internalization (red DiD) into the inflamed ECs (green) through hand-over from the monocytes (blue DiO) over time. In the time series of images during 90 min on the single inflamed EC, the hand-over process from the monocytes is done by 60 min, and another monocyte starts the process around 70 min. The automated segmentation of AI-driven image analysis exhibits approximately 70% internalization through the cell membrane out of the total liposomes **(**Fig. 1e**)**. Under the same imaging on inflamed ECs in a multi-time scale for 24 h, the significant increases of liposome internalization are visualized after 6 h, which continues afterward, as confirmed by the quantitative image analysis **(**Fig. 1f**)**.

The expression of cyclooxygenase2 (COX2; red) inside ECs (green actin and blue nucleus) significantly increases twice upon inflammatory induction in the absence of aspirin treatment **(Extended data** Fig. 2b**)**. The elevated expression is significantly reduced four times by the hand-over of aspirin-liposome from monocytes to inflamed ECs. As another validation of hand-over process, the anti-inflammatory effect of aspirin is determined through the liposome internalization into inflamed ECs **(**Fig. 1g**)**. After aspirin (19.2

μg) is encapsulated by liposomes, aspirin-liposomes are loaded into monocytes. The hand-over effect is compared with soluble treatment of aspirin by varying the concentration from 19.2 to 96 μg (1 ~ 5 fold : X) in the trans-well culture with inflamed ECs as shown in the illustration. Consequently, the COX2 expression of ECs is suppressed significantly by the liposomal hand-over (19.2 μg). The same suppression effect is seen by increasing the soluble concentration up to 5X (96 μg) although the significant suppression starts at 2X soluble treatment. Of note, when the mass of internalized aspirin is determined by liquid chromatography-mass spectrometry (LC-MS) analysis in this comparison, the hand-over enables 17.5 μg (91.1%) of cellular uptake in contrast to 3.1 μg (3.2%) of 5X soluble treatment, indicating a significant advantage of target-specific delivery.

2. Caveolin as a key receiver of the hand-over through inflammatory upregulation of expression.

Liposomes internalize into cells through i) passive diffusion, ii) actin-mediated penetration (phagocytosis and macro-pinocytosis), and iii) receptor-mediated process (clathrin and caveolin). Caveolin appears to play a key role in the hand-over process with upregulation of the expression under inflammation (Fig. 2a). As a major mediator, the caveolin expression (red) increases significantly in inflamed ECs compared to the non-inflamed condition in immunostaining with quantitative analysis (Fig. 2b **and Extended data** Fig. 3a). However, the clathrin expression is not upregulated by inflammation **(Extended data** Fig. 3b). In the same setting, inflamed hepatocytes significantly increase caveolin expression compared to the non-inflamed control as well **(Extended data** Fig. 3c).

Liposome-loaded monocytes are co-cultured with ECs in trans-wells (Fig. 2c **and Extended data** Fig. 3d). As the degree of inflammation increases in the co-culture, more monocytes (yellow box : smaller nuclei) approach ECs (bigger nuclei), indicating increases in the demand of hand-over through upregulation of caveolin expression. This result is supported by the images of super-resolution microscopy as caveolin (red) and liposome (green) colocalizes (yellow) on ECs, indicating the receiver role of caveolin in internalizing liposomes through the inflammatory hand-over (Fig. 2d). Also, the co-localization between gold-liposome and caveolin (Ω shape) on the ECs confirms their integration under the hand-over from the adjacent monocytes (Fig. 2e).

As another validation, the functions of actin, either clathrin or caveolin, and both are inhibited using cytochalasin D, active ingredient, active ingredient, and active ingredient-active ingredient, respectively, in the trans-well culture (Fig. 2f). When red (DiO) fluorescent-tagged liposomes are added, the liposomal uptake by inflamed hepatocytes significantly decreases in all inhibition groups compared to no inhibition. The inhibition of actin function least decreases the liposomal uptake among the inhibition groups, and no clear differences are seen among the inhibition of receptor-mediated functions upon immunostaining with quantitative analysis. In the same setting with EC culture (Fig. 2g), the same results are seen except the significant decrease in the synergistic inhibition of both clathrin and caveolin compared to each inhibition. However, when the degree of inflammation is increased to a strong level, the receiver role of caveolin becomes more apparent as its inhibition significantly reduces the uptake compared to the

inhibition of clathrin. The other comparison results remain in the same trends with those of weak inflammation.

These results suggest that caveolin plays a major role in the hand-over process, and this role becomes even more significant as the inflammatory severity increases. In addition, fluorescent-tagged liposomes are loaded into monocytes, which are co-cultured with inflamed ECs in trans-wells **(Extended data** Fig. 3e**)**. When the culture temperature decreases from 37 to 4 ^{o}C, the number of liposomes (red DiO) is reduced inside inflamed ECs. The result indicates the energy-dependent nature of hand-over process as the cellular energy decreases at 4 ^{o}C, and thus, the energy-required action by caveolin mediates the hand-over process rather than the energy-independent passive diffusion.

3. Anti-inflammatory effect of aspirin by hand-over to mouse inflamed sites.

As one of the two mouse models to validate the hand-over process **(**Fig. 3a**)**, the hindlimb ischemia model is used by implanting a microchannel hydrogel as a delivery bed upon blood reperfusion into inflamed ECs. First, liposomal targeting by monocyte carriers is examined by ligating the femoral artery with hydrogel implantation (Day 0), followed by tail vein injection of fluorescent-tagged liposomes (Day 1) and sacrifice (Day 7). Next, the anti-inflammatory effect of aspirin through hand-over is determined by liposomal injection (+/- aspirin) every three-day (Day 2–11) post ligation, followed by sacrifice (Day 14). In the first step, each mouse undergoes ligation and dissection of femoral vein and artery to generate ischemic hindlimb **(Extended data** Fig. 4a**)**. Laser Doppler imaging confirms the significant reduction of blood perfusion through the hindlimb as supported by the quantitative analysis. IVIS imaging exhibits the elevated signal at the hydrogel of ischemic hindlimb compared to non-target sites **(**Fig. 3b**)**.

This result is further confirmed by harvesting the hydrogel with confocal imaging post immunostaining **(**Fig. 3c**)**, which shows that monocytes (red CD11b) carry liposomes (green DiD) through microchannels (dashed line). As a validation of anti-inflammatory effect **(**Fig. 3d**)**, the aspirin hand-over reduces COX2 expression in the ischemic hindlimb compared to no aspirin at day 7 in immunostaining with quantitative analysis. This result is confirmed as the expression of other inflammatory markers (tumor necrosis factor-alpha (TNF-α) and interleukin-6 (IL-6)) significantly decreases by the aspirin hand-over compared to no aspirin in immunostaining with quantitative analysis **(**Fig. 3e**)**. Therefore, the inherent nature of monocytes upon loading of aspirin-liposome leads to efficient targeting, hand-over, and anti-inflammatory therapy in the ischemic hindlimb.

A fatty liver is used as the other model by subjecting each apoE gene knockout (apoE KO) mouse to a western diet for 6 weeks **(**Fig. 3f**)**. The weekly intravenous (IV) injection of liposome (+/- aspirin) or soluble aspirin, and the daily oral injection of aspirin are compared in the therapeutic effect on inflamed hepatocytes. Compared to no aspirin **(**Fig. 3g**)**, only the aspirin-liposome significantly reduces the COX2 expression in the fatty liver among the groups of aspirin injection in the western blot analysis. This result is supported by the same trends in the expression of TNF-α and IL-6 as other markers of inflammation in the immunostaining analysis **(**Fig. 3h **and Extended data** Fig. 4b**)**. The hand-over effect of aspirin-

liposome is further evidenced in reducing lipid accumulation and peroxidation substantially as lipotoxicity markers among the test groups (Fig. 3i **and Extended data** Fig. 4c). These results validate the therapeutic effect of hand-over on the fatty liver. Of note, the IV and oral injection of aspirin also reduce the IL-6 expression and lipid accumulation substantially compared to no aspirin.

4. Prolonged hand-over to platelets under circulation as another dual therapeutic action.

As the first action of dual therapies (Therapy 1), the anti-inflammatory therapy by hand-over has been shown so far through inherent targeting to inflamed ECs and hepatocytes by monocyte carriers of aspirin-liposome. As another dual action (Therapy 2), the prolonged anti-thrombosis therapy is approached by the hand-over of aspirin-liposome from monocytes to platelets under circulation over 7 days (Fig. 4a). As the starting point (Fig. 4b), DiD or gold-tagged liposomes are loaded into monocytes, which are then incubated with platelets for 3 h in vitro. When DiD-tagged liposomes are detected in FACS (Fig. 4c), 73.2% platelets out of the total (100%) in the culture uptake liposomes upon hand-over from monocytes. This outcome is confirmed by visualizing the circular localization of gold dots (10 nm, see the scale bar) under TEM as a presentation of liposomal uptake by a platelet (Fig. 4d). These results validate the hand-over from monocytes into platelets.

Fluorescent-tagged liposomes are injected into a tail vein of each mouse (**Extended data** Fig. 5a). Then, cells are harvested from spleen as a major residence of monocytes, followed by selective sorting of monocytes (top tubes) from other cells (bottom tubes). When the fluorescence intensity of each tube is determined in IVIS, the monocytes exhibit 75% liposome (+) signals out of the total cells, which is maintained for 7 days, indicating the prolonged liposomal loading to splenic monocytes. Next, the in vivo action to suppress platelet activation is examined by tail vein injection of aspirin-liposome in comparison with oral injection of aspirin, followed by collecting blood and activating platelets in culture (Fig. 4e). Next, splenectomy is carried out as a depletion control of splenic monocytes so that the carrier role of monocytes in the hand-over to circulating platelets can be validated.

Within a short-term (1.5 h) post injection in comparison with no aspirin (Fig. 4f), oral aspirin injection and IV aspirin-liposome injection significantly decreases the platelet activation in FACS analysis of CD62p expression as a representative marker of platelet activation. The same trend is seen from day 3 to 7 with significantly incremental reductions from oral aspirin injection to IV injection of aspirin-liposomes (Fig. 4g). The splenectomy significantly attenuates the anti-platelet effect compared to the intact hand-over at day 7 because the carrier function of splenic monocytes is absent (Fig. 4h). This result is confirmed when platelets are isolated from these mice (Day 7) and subjected to imaging of platelet morphologies by scanning electron microscopy (SEM) with quantitative analysis (Fig. 4i). The splenectomy results in the typical morphologies of activated platelets with rough surface and elongated pseudopodia as opposed to the morphologies of intact hand-over. These results indicate the anti-platelet effect from the prolonged circulation of aspirin-liposome upon loading to splenic monocytes. Platelets are isolated from the mice post injection of fluorescent-tagged liposomes and subjected to IVIS analysis

(Fig. 4j). The effect of splenectomy is not seen on day 3 but becomes apparent on day 7 in attenuating the anti-platelet effect, indicating the monocyte dependency of prolonged therapeutic action.

Hence, the hand-over from monocytes to platelets is expected to last over 7 days **(Extended data** Fig. 5b**)**. In contrast, the direct targeting effect is also determined using activated platelets upon thrombin treatment in vitro, followed by co-incubation with liposome, aspirin, or aspirin-liposome in comparison for 1 h **(Extended data** Fig. 5c**)**. The SEM images indicate platelet activation is significantly reduced by aspirin regardless of liposome encapsulation compared to only liposome treatment. This result is confirmed by the quantitative image analysis of pseudopodia length as a marker of spreading platelet activation. Platelets are activated by culturing on collagen-coated plates as a model of basement exposure upon dysfunction of blood vessels, followed by incubation with phosphate-buffered saline (PBS), aspirin, or aspirin-liposome in comparison for 1 h **(Extended data** Fig. 5d**)**. The expression of activation marker (red CD62p) in platelets (green CD41) is significantly reduced from PBS to aspirin only and aspirin-liposomes as confirmed by the quantitative image analysis of platelet aggregation. These results indicate that aspirin-liposomes can target platelets directly through delivery by blood flow as the body clearance of nanoparticles usually occurs within 3 days.

5. Targeted and multi-organ therapies by dual actions of hand-over on atherosclerosis.

Atherosclerosis is induced in a carotid artery by subjecting apoE KO mice to western diet for 42 days with partial ligation of the artery by surgery on day 14. The weekly tail vein injection of liposomes (+/- aspirin) is compared with the daily oral injection of aspirin (Fig. 5a). Splenectomy is conducted on day 40 with injection of fluorescent- tagged liposomes on day 41 with IVIS analysis (Fig. 5b). The intact mice exhibit the majority of liposomal distribution into spleen and liver whereas the splenectomy mice show no splenic distribution with the strong and weak signals in liver and lung, respectively. The splenectomy results in nearly no targeting to the ligated carotid artery under inflammation in addition to the relatively weak signal in the non-ligated artery as well due to the depletion of splenic monocytes (Fig. 5c). In contrast, the intact mice exhibit more positive signals of liposomal distribution in the ligated artery compared to the non-ligated control, indicating the carrier role of splenic monocytes in the hand-over to the inflamed artery.

In the same model, gold-tagged liposomes are injected on day 35 with analyses by inductively coupled plasma-mass spectrometry (ICP-MS) (day 35, 36, 38, and 42) and TEM analyses (day 38) **(Extended data Fig. 6a)**. The dominant distributions to the liver and spleen are resulted. Compared to the liver as set to 100%, the splenic distribution reaches 17.11% as an indication of efficient liposomal targeting to spleen for 3 days compared to the other organs except the liver in the table. It is turned out that the spleen targeting of gold-liposomes increases from day 0 to 3 (17.11%), which is maintained to 11.51% until day 7. Under TEM imaging (Fig. 5d), monocytes, foam cells (lipid-laden cells originated from monocytes), and ECs exhibit intracellular gold nanoparticles as evidence of targeted hand-over to the atherosclerotic artery. At day 3 post injection, the hand-over of gold-liposomes to dysfunctional ECs is visualized under TEM imaging **(Extended data Fig. 6b)**. Aortic arch is naturally exposed to disturbed flow, and thus, ECs increase

the permeability as an indication of dysfunction. Gold-liposomes are found inside foam cells and ECs, indicating the efficient delivery of liposomes to dysfunctional ECs as a therapeutic target.

Due to the dual actions of hand-over therapy, the expression of inflammatory markers (COX2, TNF-α and IL-6) significantly decrease in the ligated carotid artery from no aspirin to oral aspirin injection and further to aspirin hand-over by immunostaining **(**Fig. 5e **and Extended data Fig. 7a)**. Only the TNF-α expression is not significantly different between the no aspirin and oral aspirin injection. The same trends are confirmed in the liver with the significant reductions of lipid droplets by the dual action therapy in hematoxylin and eosin (H&E) staining **(**Fig. 5f**)**. The therapeutic effects of dual action are also evidenced in the blood with significant decreases of total cholesterol, low-density lipoprotein, and triglyceride levels **(**Fig. 5g**)** in addition to the prostaglandin E2 (PGE2) levels as a blood inflammation marker **(**Fig. 5h**)**.

These multi-organ effects cooperate to suppress atherosclerosis of ligated carotid artery as the lesion formation significantly decreases from no aspirin to oral aspirin injection and further to the aspirin hand-over in the H&E analysis **(**Fig. 5i**).** As a supportive result **(Extended data Fig. 7b)**, the aspirin hand-over exhibits the normal (non-inflammation and no aspirin)-like histological features of inflamed arteries. In contrast, no aspirin and aspirin oral result in nearly complete and partial stenotic features of inflamed arteries, respectively. Next, the biosafety profile of aspirin-liposome is examined in the liver where most dominant distribution is detected **(Extended data Fig. 7c)**. The aspirin-liposome does not cause hepatotoxicity as evidenced by no significant elevation of marker expression including aspartate aminotransferase (AST), alanine aminotransferase (ALT), gamma-glutamyl transferase (GGT) and alkaline phosphatase (ALP) from blood samples. This result is supported by no visible finding of abnormal H&E features in spleen, lung, kidney, intestine, and heart **(Extended data Fig. 7d)**.

Conclusion

The drug effect should be focused on target cells accurately, which also require propagation to cover the neighboring pathogenic area effectively. This study suggests a translatable strategy in response to this requirement by using not only inflammation-triggered natural targeting of splenic monocytes but also the intercellular hand-over mechanism. As a notable point, the uses of liposome and aspirin serve as a lay language tool to amplify the impact of strategy. As cells communicate with neighbors by tossing and receiving molecules, the drug effect can be delivered from cell to cell through a hand-over mechanism. The significance of present study lies in validating caveolin as a major mediator of the hand-over process in collaboration with clathrin. Caveolin increases the expression to handle the elevated demand of hand-over as inflammation initiates, and the severity increases. In this regard, this study suggests a considerable means to potentiate the anti-inflammatory effect from targeted treatment of drugs by upregulating the caveolin expression.

Stimuli-responsive targeting and release have been a major paradigm in current drug treatment to avoid systemic side effects[13, 26]. So far, the technical development has been first focused on the advanced design of delivery vehicles by adding pH[27], reactive oxygen species (ROS)[28], or enzyme-responsive

properties[29]. Second, pin-point targeting has been approached by relying on unique molecule-molecule interactions[30, 31]. Third, a specific condition-mediated exertion of effect has been strategized in response to activation of inflammatory[32, 33], immune[13], or cancer cells[34]. Although continuous progress has been made, none of these methods has reached the level of enough success in clinics. This study approaches spontaneous targeting of monocytes from splenic residency like a stimuli-responsive fashion to deliver the drug through caveolin-mediated endocytosis in a means of receptor-ligand interaction.

Moreover, the drug effect is focused on the cells in the inflammation-specific condition. In this way, our strategy covers the three strategies of current drug development by simply injecting drug-liposome through a vein. Together with these step-by-step controls using the body-responses, the caveolin action provides cascadic regulations to minimize potential errors in drug treatment like thrombosis and complement pathways which are involved with many regulatory factors and steps. These aspects of strategy represent a promising potential for clinical translation without having any complex factor by simply utilizing the inter-body operations.

The aspirin effects have been separately used so far to either anti-inflammation or anti-platelet therapy in the clinics[20–23]. Unlike drug repositioning to treat a different disease, this study suggests a dual therapy by combining both effects of aspirin considering the safety from uses over a century. The dual therapeutic effects are generated by simple liposomal encapsulation of aspirin with venous injection rather than oral intake, which also prolongs the effects by monocyte carrying through systemic circulation. These easy but translatable approaches represent as another selling point for the drug industry. Moreover, because atherosclerosis is considered as an uncurable disease for the past decades, the efficacy and safety of aspirin-liposome suggest a promising therapy to investigate further in the clinical setting.

As technical methods to emphasize here, 3D high-resolution time-series imaging with lattice light-sheet microscopy[35] and super-resolution imaging with AI segmentation analysis[36] are utilized to capture the details of hand-over process. Nonetheless, intracellular process of aspirin-liposomes post caveolin-mediated endocytosis needs to be studied further. Also, although the mouse models are reliable to study the hindlimb ischemia, fatty liver, and atherosclerosis, a large animal model should be employed in the next study. Most results track liposomes and aspirin effects rather than aspirin itself as there is no way to label aspirin using current techniques, which also requires a further study. As seen in liposomal uses of COVID-19 vaccines[37] and bleeding by long-term use of aspirin[25], other side effects need to be checked more thoroughly in the next study.

Methods

1. Liposome preparation

An aspirin solution was prepared by dissolving aspirin (A5376, Sigma-Aldrich, St. Louis, MO, USA) in ethanol (5 mg/mL). Three liposomal compositions were dissolved in ethanol (E7023, Sigma-Aldrich) at

72°C using a molar ratio of 55:40:5 in dipalmitoyl phosphatidylcholine (850355P, Sigma-Aldrich), cholesterol (C8667, Sigma-Aldrich), and 1,2-dysteroyl-sn-glycero-3-phosphoethanolamine-N-[methoxy (polyethylene glycol)] (880120P, Sigma-Aldrich), followed by vigorous stirring at 500 revolutions per minute (RPM) at 72°C for 5 min. Then, aspirin-liposomes are produced through rapid injection of the aspirin solution with a quadruple volume into the liposomal mixture using a needle syringe (20 G; Restek, Bellefonte, PA, USA) under the vigorous stirring condition for 15 min at room temperature.

The solution was then filtered, dialyzed, and centrifugated to collect aspirin-liposomes by controlling the size. Briefly, the solution was passed through three filters in the order of drain disc (PETEDD9025, Sterlitech, Auburn, WA, USA), 0.1 μm membrane filter (PCT019030, Sterlitech), and another drain disc. This process was repeated 7 times using an extruder (GOE-1000mL, Genizer, Irvine, CA, USA) and a peristaltic pump (BT100L, Lead Fluid Technology, Heibei, China) with a flow rate of 25 mL/min. Dialysis was carried out using a membrane to cut off 12–14 kDa (132678T, Repligen, Waltham, MA, USA) in phosphate-buffered saline (PBS; LB004-02, Welgene, Seoul, Republic of Korea) for 24 h so that residual aspirins were removed. Aspirin-liposomes were collected through centrifugation at 30,000 g for 1 h, followed by resuspension in PBS or normal saline (JW Pharmaceutical, Seoul, Republic of Korea) for experimental uses.

Aspirin-free liposomes or gold-liposomes were prepared by replacing the aspirin solution with PBS or a solution of gold nanoparticle (10 nm in diameter; 752584, Sigma-Aldrich). Liposomes were tagged with DiD (V22887, Thermo Fisher, Waltham, MA, USA) or DiO (V22886, Thermo Fisher) following the manufacturer's instructions.

2. Liposome characterization

The liposomal quantity was determined using the Stewart assay[38]. Briefly, liposomes and standard lipid samples were dissolved in chloroform (6955, Duksan, Ansan, Republic of Korea). Each lipid sample was reacted with a ferrothiocyanate reagent which was prepared by dissolving ferric chloride hexahydrate (27.03 g; F2877, Sigma-Aldrich) and ammonium thiocyanate (30.4 g; 221988, Sigma-Aldrich) in deionized water (1 L). The reacted solution was mixed under vigorous vortex for 20 sec and then centrifuged at 300 g for 10 min for phase separation. The absorbance (485 nm) of lower phase was measured using a UV-visible spectrophotometer (Lambda 25, Perkin Elmer, Waltham, MA, USA).

Liposome morphology and size distribution were examined using transmission electron microscopy (TEM; Jem2100, JEOL, Tokyo, Japan) and dynamic light scattering (DLS; ELS-Z1000, Otsuka Electronics Ltd., Tokyo, Japan). The aspirin amount in liposomes was quantified using liquid chromatography-mass spectrometry (LC-MS; Q-exactive orbitrap plus, Thermo Fisher).

3. Animal experiment

All animal experiments were conducted according to the guidelines and protocols approved by the Institutional Animal Care and Use Committee of Yonsei University College of Medicine (Permit No. 2019 –

0205, 2022-0050). Male mice (6 weeks-old C57BL/6) with either normal (Orient Bio, Gyeonggi-do, Republic of Korea) or apoE gene knockout (apoE KO; SLC, Shizuoka, Japan) were used until sacrifice under CO_2.

Mice were anesthetized through intraperitoneal injection of zoletil (50 mg/kg; Virbac, Seoul, Republic of Korea) and xylazine (10 mg/kg; Bayer, Leverkusen, Germany). A feeding needle catheter (22 G x 25 mm; NC9924986, Thermo Fisher) and syringe (29 G; U-100, Terumo, Tokyo, Japan) were used for oral and tail vein injection, respectively. A total of 350 μg aspirin was administered per week after dissolving in normal saline (200 μL) with 1% ethanol by daily oral injection of 50 μg for seven days or one-day intravenous (IV) administration of 350 μg. In contrast, the anti-platelet effect was examined by one-shot injection of 350 μg regardless of mouth or tail vein.

Mice were subjected to organ harvesting or blood collecting after anesthetizing and exposing the heart. Organs were harvested after perfusing active ingredient (100 IU/kg; JW Pharmaceutical) in cold normal saline (10 mL) through left ventricle with cutting of the inferior vena cava. Blood was collected through cardiac puncture using active ingredient-coated tubes (454322, Greiner Bio-One, East Centre, Singapore), followed by adding GPRP peptide (0.4 mM; CAS 67869-62-9, Calbiochem, San Diego, CA, USA) to prevent coagulation.

4. Cell culture

Monocytes were isolated from the spleen of C57BL/6 mice using a CD11b selection kit (480110, BioLegend, San Diego, CA, USA) following the manufacturer's protocol. The monocytes were then seeded (1×10^7 cells/mL) and cultured in RPMI 1640 medium (11875-093, Thermo Fisher) supplemented with fetal bovine serum (FBS; 10% v/v, 16000–044, Thermo Fisher) and active ingredient–active ingredient (1% v/v; 15140-122, Thermo Fisher) with 5% CO_2 at 37°C.

As an endothelial cell (EC) model, human umbilical vein endothelial cells (HUVECs; Lonza, Basel, Switzerland) or red fluorescent HUVEC (Lonza) were seeded (1×10^5 cells/mL) and cultured in EGM-2 Bullet Kit medium (CC-3162, Lonza). As a hepatocyte model, HepG2 cells (Korean Cell Bank, Seoul, Korea) were seeded (5×10^4 cells/mL) and cultured in minimum essential media (11095-080, Invitrogen, Carlsbad, California, USA) supplemented with FBS (10% v/v) and active ingredient–active ingredient (1% v/v).

Platelets were isolated from the blood post collection following the process above. Briefly, the blood (200 μL) was diluted with PBS (500 μL) and then centrifuged at 100 g for 10 min with no break in the deceleration step, thereby producing the platelet-rich plasma in the supernatant. This plasma was mixed with an equal volume of PBS and centrifuged at 800 g for 20 min with no break in the deceleration step, followed by resuspension in PBS for experimental uses.

5. Liposome loading into monocytes with validation

Liposomes (+/- aspirin, tagged with fluorescence or gold) were injected into the tail vein of each mouse so that these liposomes are loaded into monocytes. Monocytes were then isolated from the mice at day 1, and in vivo imaging system (IVIS; 124262, Perkin Elmer) was used to determine the liposomal

distribution to each organ and to splenic monocytes. The results were validated using the isolated monocytes by fluorescence-activated cell sorting (FACS; as described below), TEM, and immunostaining (as described below) with anti-CD11b-FITC (1:200; MA1-10081, Thermo Fisher).

6. In vitro hand-over from monocyte to EC, hepatocyte, and platelet

Trans-wells (3422, Corning, New York, NY, USA) with pore of size 8.0 μm were used to co-culture monocytes (upper chamber) and ECs (lower chamber) for 24 h (if not otherwise specified). ECs were activated by treating lipopolysaccharide (LPS; L4391, Sigma-Aldrich) with 0.1 and 1 μg/mL to reach the weak and strong levels, respectively. The hand-over to inflamed ECs was examined through immunostaining or TEM imaging with gold-tagged liposomes. Aspirin-liposome (19.2 μg per well / 24-well plate) was treated on inflamed ECs, which was compared to the soluble aspirin treatment (19.2, 38.4, or 96 μg per well / 24-well plate), followed by determining the aspirin uptake by inflamed ECs using LC-MS. Inflamed ECs were immune-stained with anti-cyclooxygenase 2 (COX2) (1:1,000; ab179800, Abcam, Cambridge, MA, USA) and secondary anti-rabbit Alexa Fluor 488 (1:500; Jackson Lab, Bar Harbor, ME, USA).

The energy-dependency of hand-over was determined in the trans-well at 4°C versus 37°C for 6 h with immunostaining (as described below). The receiver roles of actin, caveolin and clathrin in hand-over were validated by treating inflamed ECs with the corresponding inhibitors including cytochalasin D (for actin; 0.1 μM; 8273, Sigma-Aldrich), active ingredient(for caveolin; 50 μg/mL; N6261-500KU, Sigma-Aldrich), or active ingredienthydrochloride (for clathrin; 25 μM; C8138-5G, Sigma-Aldrich). All inhibitors were treated using a solution in 0.1% dimethyl sulfoxide (S-002-M, Merck, Burlington, MA, USA), and monocytes were co-cultured with those ECs under 30 min treatment of inhibitor, followed by immunostaining after 24 h of co-culture.

High-resolution time series of 3D images were obtained by lattice light-sheet microscopy (Lattice Lightsheet 7, Carl-Zeiss, Oberkochen, Germany) with subsequent analysis using an artificial intelligence (AI)-driven automated segmentation program (Arivis, Carl-Zeiss). Super-resolution microscopy (Elyra 7, Carl-Zeiss) was used to confirm the co-localization of liposome and caveolin upon staining with anti-caveolin (1:50; arg57976, arigo Biolaboratories Corp, Hsinchum, Taiwan) and secondary anti-rabbit Alexa Fluor 594 (1:500). The expression of caveolin and clathrin in ECs under LPS treatment was evaluated without monocytes co-culture upon immunostaining with anti-caveolin (1:50), anti-clathrin (1:50; D3C6, Cell Signaling Technology, Danvers, MA, USA), and secondary anti-rabbit Alexa Fluor 488 (1:500).

Hepatocytes were cultured in the trans-well system under treatment of ethanol (1%) with parafilm (P7793, Sigma-Aldrich) sealing to set up an inflammatory condition. As inhibitors, cytochalasin D (for actin; 2 μM), active ingredient(for caveolin; 50 μg/mL), or active ingredient hydrochloride (for clathrin; 50 μg/mL) was used. Platelets were incubated with monocytes for 3 h in centrifuge tubes (MCT-175-C, Corning), followed by TEM with gold-liposomes and FACS analysis upon immunostaining with anti-CD41-FITC (1:2,000; MA1-80666, Invitrogen).

7. Mouse hindlimb ischemia

Each mouse underwent ligation of femoral artery with implantation of microchannel hydrogel. The hydrogel was produced by crosslinking gelatin (5.5% w/v in PBS; G1890, Sigma–Aldrich) with microbial transglutaminase (mTG; 10% w/v in PBS; 1203-50, Modernist Pantry LLC, Eliot, ME, USA) in a formulation of gelatin/mTG solution (9:1 ratio, final concentration = 5% w/v). As sacrificing materials, poly(N-isopropylacrylamide) (PNIPAM;535311, Sigma-Aldrich) fibers were prepared using a custom-made spinning device (2,500-2,800 RPM) with PNIPAM (53% w/v) in methanol solution (67-56-1, Merck) and placed in a mold (4 × 4 × 3 mm) at a density of 11.45 ± 3.13 μg/mm^3. In this way, threads of PNIPAM fibers were embedded in the gelatin/mTG hydrogel to generate microchannel networks after pouring the hydrogel solution into the mold as reported previously[13]. PNIPAM fiber was then melted with cold PBS by inducing gel-to-sol transition, followed by perfusion washing. The hydrogel served as a bed of liposomal tracking and hand-over analysis as the microchannel networks enabled perfusion connection with surrounding vessels.

After each C57BL/6 mice was anesthetized with skin incision, the upper and lower points of femoral artery were ligated in the left hindlimb using a 6 − 0 black silk (SK517, Ailee), followed by resecting the blood vessels between the two points. The microchannel hydrogel was implanted in both hindlimbs, and the skin was closed using a 4 − 0 black silk (SK434, Ailee). Laser Doppler imaging (moorLDLS2, Moor Instruments, Devon, UK) confirmed cessation of blood flow in the ischemic hindlimb. The hand-over process and anti-inflammatory effect on the inflamed sites were examined by injecting liposomes through tail vein with IVIS tracking. The microchannel hydrogel was harvested for immunostaining using anti-COX2 (1:1,000), anti-tumor necrosis factor-alpha (TNF-α) (1:1,000; 3707, Cell Signaling Technology), anti-interleukin-6 (IL-6) (1:200; NB600-1131, Novus, Centennial CO, USA), and secondary anti-rabbit Alexa Fluor 488 (1:500).

8. Mouse fatty liver

The fatty liver model was produced by feeding apoE KO mice with the western diet (D12079B, Research Diets, New Brunswick, NJ, USA) for 42 days. Soluble aspirin and liposomes (+/- aspirin) were injected daily through the mouth or weekly through the tail vein, respectively. The liver was harvested and subjected to immunostaining using anti-TNF-α (1:1,000), anti-IL-6 (1:200), AdipoRed assay reagent (PT-7009, Lonza), anti-reactive oxygen species 581/591 (1:200; D3861, Thermo Fisher), and secondary anti-rabbit Alexa Fluor 488 (1:500).

Western blotting was carried out by treating the liver tissues with RIPA buffer (R0278, Sigma-Aldrich) on ice to extract total proteins, followed by centrifugation at 13,200 RPM for 30 min and BCA protein assay (23227, Thermo Fisher) to determine the protein concentration. The proteins (25 μg) were separated on a 10% SDS-polyacrylamide Mini-PROTEAN TGX gel (456–1084, Bio-Rad Laboratories, Hercules, CA, USA) and electrotransferred onto a nitrocellulose membrane using iBlot 2 NC gel regular stacks (IB23001, Invitrogen). The membrane was blocked in 1X tris-buffered saline with tween-20 (TBST) buffer (BTT-

9110, T&L, Seoul, Republic of Korea) with 5% non-fat dry skim milk (1706404, Bio-Rad Laboratories) containing 0.1% tween-20 (P9416, Sigma-Aldrich) for 1 h at room temperature.

The membranes were incubated at 4°C overnight with primary mouse anti-COX2 (1:1,000) and mouse anti-actin (1:1,000; sc-47778, Santa Cruz, Dallas, TX, USA) antibodies after dilution in 5% skim milk with TBST. Then, the membranes were washed with 1X TBST three times (each for 15 min) and incubated with secondary goat anti-rabbit IgG(H + L)-horseradish peroxidase (HRP) conjugated (1:5,000; 31460, Thermo Fisher) or goat anti-mouse IgG(H + L)-HRP conjugated (1:5,000; 31430, Thermo Fisher) antibodies for 1 h. After washing three times with 1X TBST, the blot signals were visualized using a western enhanced chemiluminescence (ECL) substrate (170–5060, Bio-Rad Laboratories) according to the manufacturer's instructions and analyzed using luminescent image analyzer (LAS-3,000; 111901, Fuji Film, Tokyo, Japan), followed by quantitative analysis with normalization to the intensity of actin.

9. Anti-platelet effect in mouse

The anti-platelet effects in mouse blood were compared among oral aspirin, IV liposomes, and IV aspirin-liposomes. As the spleen is a major reservoir of monocytes, splenectomy was conducted to inhibit the reservoir function one day before injection. Each mouse underwent anesthetization and skin incision with anatomical scissors, and the main arteries and veins of splenic ligament were tied using 6 – 0 black silk, followed by removing the entire spleen upon cutting the distal blood vessels at the tied-off points. The platelets were prepared as described above and activated by thrombin (372 μM; 10602400001, Sigma-Aldrich) treatment for 10 min or culturing on collagen (100 μg/mL; C7521, Sigma-Aldrich)-coated plates for 30 min. Then, platelet analyses were carried out by FACS, scanning electron microscopy (SEM; Carl-Zeiss), IVIS, or immunostaining with anti-PE-CD62p (1:2,000; 12-0626-82, Invitrogen) and anti-FITC-CD41 (1:2,000).

10. Mouse vascular atherosclerosis

ApoE KO mice were fed with western diet for 42 days, and partial carotid ligation was conducted at day 14 as reported previously[30]. Briefly, three out of four branches from the left common carotid artery were ligated using 10 – 0 sutures (W2814, Ethicon, Raritan, NJ, USA), followed by closing skin with 6 – 0 vicryl sutures (J510G, Ethicon). The liposomal distributions were determined using IVIS after injecting fluorescent-tagged liposomes at day 41 with or without splenectomy. Gold-liposomes were injected at day 35, and each organ was harvested, followed by determination of gold concentration and location by inductively coupled plasma-mass spectrometry (ICP-MS; Nexion 2000, Perkin Elmer) and TEM, respectively. Blood was collected from each mouse, and the prostaglandin E2 level was determined using enzyme-linked immunosorbent assay kit (ab133021, Abcam) following the manufacturer's instructions. The levels of lipotoxicity or hepatotoxicity markers were determined using an automated clinical chemistry analyzer (FUJI DRI-CHEM NX500i, Fuji Film). Immunostaining was carried out using harvested tissues with anti-COX2 (1:1,000), anti-TNF-α (1:1,000), anti-IL-6 (1:200), and secondary anti-rabbit Alexa Fluor 488 (1:500).

11. Immunostaining and FACS

In vitro samples were fixed with 4% paraformaldehyde (CNP015-0500, CellNest, Hanam, Republic of Korea), permeabilized with 0.2% Triton X-100 (93443, Sigma-Aldrich), and blocked with 5% bovine serum albumin (BSA; 82-100-6, Merck). In vivo samples were fixed in 10% neutral-buffered formalin (FR2013-100-00, Biosesang, Gyeonggi, Republic of Korea) and embedded in paraffin, which were sectioned to 4 μm thickness, deparaffinized, and rehydrated. Samples were incubated with primary antibodies at 4°C overnight, washed with PBS three times, and incubated with secondary antibodies at room temperature for an hour. After counterstaining with DAPI (H1200, Vectashield, Darmstadt, Germany) and phalloidin (A12379, Thermo Fisher), confocal imaging was carried out with analysis using ZEN software V3.0 (Carl-Zeiss) or ImageJ (NIH, Bethesda, MD, USA).

COX2 immunostaining was carried by deparaffinizing and rehydrating the sections with antigen retrieval by incubating in low-pH buffer (K8005, Agilent Dako, Santa Clara, CA, USA) at 95°C for 20 min. Endogenous peroxidases were inactivated through incubation in 3% H_2O_2 (7722-84-1, Sigma-Aldrich) solution for 10 min, followed by TBST washing and blocking with 5% BSA in PBS. Samples were then incubated with anti-COX2 (1:1,000) at room temperature for 1 h and then with a secondary HRP-labeled polymer anti-rabbit antibody (K4003, Agilent Dako) at room temperature for 20 min. 3,3'-diaminobenzidine (DAB) development solution (K3468, Agilent Dako) was added to the samples for 5 min, followed by washing with distilled water, counterstaining with hematoxylin (K8008, Agilent Dako), and optical imaging (Leica DMi8, Leica Microsystems, Wetzlar, Hesse, Germany).

FACS analysis was carried by incubating cells with antibodies for 1 h at room temperature, followed analysis with a flow cytometer (LSR Fortessa, BD Bioscience, Mississauga, Canada) and FlowJo software (V10, BD Bioscience).

12. Statistical analysis

Data were collected from multiple independent experiments, and each n number was denoted in the corresponding figure legend. All data points (represented as circles, triangles, or squares) were displayed in the graphs when the sample size is less than 10. Statistical analyses were performed using GraphPad Prism (GraphPad Software, San Diego, CA, USA). A two-tailed Student's t-test was utilized to compare the two groups. For multiple group comparisons, a one-way analysis of variance was conducted, followed by Tukey's post-hoc test for pairwise comparisons. Statistical significance was set at a p-value of less than 0.05. P-values were denoted in the figures as *, **, and *** for $p < 0.05$, $p < 0.01$, and $p < 0.001$, respectively, with dashed lines indicating the groups in comparison. The data were presented as mean ± standard error of the mean (SEM), with units of measurement.

Declarations

Acknowledgments

The research was supported by Korean government grants, including i) from the Korean Fund for Regenerative Medicine (KFRM) grant funded by the Korean government (the Ministry of Science and ICT,

the Ministry of Health & Welfare with the code in KFRM 23A0203L1), ii) from the National Research Foundation of Korea (NRF) grant funded by the Korea government (MSIT: RS-2023-00248656), and iii) from the National Research Foundation of Korea (NRF) Grant funded by the Korean Government (MSIT: NRF-RS-2023-00207857). The authors acknowledge training supports from the MD-PhD/Medical Scientist Training Program through the Korea Health Industry Development Institute (KHIDI) funded by the Ministry of Health & Welfare, Republic of Korea and the Brain Korea 21 PLUS Project for Medical Science of Yonsei University

Author contributions

S.E.Y. and J.K. contributed equally to this work as the co-first authors. S.C. and H.-J.S. (lead) are listed as the co-corresponding authors considering their guidance and organization of entire work. S.E.Y. and S.C. planned and managed most experiments; S.E.Y., J.K. and S.C. contributed to data acquisition and analysis; D.-H.K. conducted mouse surgeries for disease modeling; S.B. and S.P. worked on the mouse models with data acquisition and analysis. H.-J.S. wrote the manuscript with assistance from S.E.Y., J.K., and S.C.

Conflict of Interest

The authors declare no competing financial interest.

References

1. Blanco, E., Shen, H. & Ferrari, M. Principles of nanoparticle design for overcoming biological barriers to drug delivery. Nature Biotechnology 33, 941–951 (2015).
2. Wilhelm, S. et al. Analysis of nanoparticle delivery to tumours. Nature Reviews Materials 1, 16014 (2016).
3. Schmidt, C.K., Medina-Sánchez, M., Edmondson, R.J. & Schmidt, O.G. Engineering microrobots for targeted cancer therapies from a medical perspective. Nature Communications 11, 5618 (2020).
4. Rosenblum, D., Joshi, N., Tao, W., Karp, J.M. & Peer, D. Progress and challenges towards targeted delivery of cancer therapeutics. Nature Communications 9, 1410 (2018).
5. Liu, J., Liu, Z., Pang, Y. & Zhou, H. The interaction between nanoparticles and immune system: application in the treatment of inflammatory diseases. Journal of Nanobiotechnology 20, 127 (2022).
6. Qu, L. et al. Caveolin-1 identified as a key mediator of acute lung injury using bioinformatics and functional research. Cell Death Dis 13, 686 (2022).
7. Yokomori, H. et al. Elevated expression of caveolin-1 at protein and mRNA level in human cirrhotic liver: relation with nitric oxide. J Gastroenterol 38, 854–860 (2003).
8. Catalan, V. et al. Expression of caveolin-1 in human adipose tissue is upregulated in obesity and obesity-associated type 2 diabetes mellitus and related to inflammation. Clin Endocrinol (Oxf) 68,

213–219 (2008).
9. Codrici, E. et al. Caveolin-1-Knockout Mouse as a Model of Inflammatory Diseases. *J Immunol Res* 2018, 2498576 (2018).
10. Xue, Y. et al. Caveolin-1 accelerates hypoxia-induced endothelial dysfunction in high-altitude cerebral edema. Cell Commun Signal 20, 160 (2022).
11. Wang, Y. et al. Effects of ethanol on the expression of caveolin-1 in HepG2 cells. Mol Med Rep 11, 4409–4413 (2015).
12. Bucci, M. et al. In vivo delivery of the caveolin-1 scaffolding domain inhibits nitric oxide synthesis and reduces inflammation. Nature Medicine 6, 1362–1367 (2000).
13. Chung, S. et al. In Situ Reprogrammings of Splenic CD11b + Cells by Nano-Hypoxia to Promote Inflamed Damage Site-Specific Angiogenesis. Advanced Functional Materials 33 (2023).
14. Senders, M.L. et al. Probing myeloid cell dynamics in ischaemic heart disease by nanotracer hot-spot imaging. Nat Nanotechnol 15, 398–405 (2020).
15. Deprez, J. et al. Transport by circulating myeloid cells drives liposomal accumulation in inflamed synovium. Nat Nanotechnol (2023).
16. Che, J. et al. Neutrophils Enable Local and Non-Invasive Liposome Delivery to Inflamed Skeletal Muscle and Ischemic Heart. Adv Mater 32, e2003598 (2020).
17. Bronte, V. & Pittet, M.J. The spleen in local and systemic regulation of immunity. Immunity 39, 806–818 (2013).
18. Lewis, S.M., Williams, A. & Eisenbarth, S.C. Structure and function of the immune system in the spleen. Sci Immunol 4 (2019).
19. Warner, T.D. & Mitchell, J.A. Cyclooxygenase-3 (COX-3): filling in the gaps toward a COX continuum? Proc Natl Acad Sci U S A 99, 13371–13373 (2002).
20. Husain, S., Andrews, N.P., Mulcahy, D., Panza, J.A. & Quyyumi, A.A. Aspirin improves endothelial dysfunction in atherosclerosis. Circulation 97, 716–720 (1998).
21. Monobe, H., Yamanari, H., Nakamura, K. & Ohe, T. Effects of low-dose aspirin on endothelial function in hypertensive patients. Clin Cardiol 24, 705–709 (2001).
22. Hohlfeld, T. & Schror, K. Antiinflammatory effects of aspirin in ACS: relevant to its cardiocoronary actions? Thromb Haemost 114, 469–477 (2015).
23. Dzeshka, M.S., Shantsila, A. & Lip, G.Y. Effects of Aspirin on Endothelial Function and Hypertension. Curr Hypertens Rep 18, 83 (2016).
24. Hartwig-Otto, H. Pharmacokinetic considerations of common analgesics and antipyretics. Am J Med 75, 30–37 (1983).
25. Jones, W.S. et al. Comparative Effectiveness of Aspirin Dosing in Cardiovascular Disease. N Engl J Med 384, 1981–1990 (2021).
26. Lin, C., Liang, Y., Guo, M., Saw, P.E. & Xu, X. Stimuli-responsive polyprodrug for cancer therapy. Materials Today Advances 15, 100266 (2022).

27. Feng, Q., Wilhelm, J. & Gao, J. Transistor-like Ultra-pH-Sensitive Polymeric Nanoparticles. Accounts of Chemical Research 52, 1485–1495 (2019).
28. Block, M.L., Zecca, L. & Hong, J.S. Microglia-mediated neurotoxicity: Uncovering the molecular mechanisms. Nature Reviews Neuroscience 8, 57–69 (2007).
29. Baig, M.H. et al. Enzyme targeting strategies for prevention and treatment of cancer: Implications for cancer therapy. Seminars in Cancer Biology 56, 1–11 (2019).
30. Yu, S.E. et al. Nanotheranostics of Pre-Stenotic Vessels By Target Touch-On Signaling of Peptide Navigator. Advanced Functional Materials 32 (2021).
31. Yoon, S.J. et al. Tissue Niche Miniature of Glioblastoma Patient Treated with Nano-Awakeners to Induce Suicide of Cancer Stem Cells. Adv Healthc Mater 11, e2201586 (2022).
32. Yazdi, A.S. et al. Nanoparticles activate the NLR pyrin domain containing 3 (Nlrp3) inflammasome and cause pulmonary inflammation through release of IL-1α and IL-1β. *Proceedings of the National Academy of Sciences* 107, 19449–19454 (2010).
33. Gupta, G. et al. Exploiting Mass Spectrometry to Unlock the Mechanism of Nanoparticle-Induced Inflammasome Activation. ACS Nano 17, 17451–17467 (2023).
34. Fan, D. et al. Nanomedicine in cancer therapy. Signal Transduction and Targeted Therapy 8, 293 (2023).
35. Chen, B.-C. et al. Lattice light-sheet microscopy: Imaging molecules to embryos at high spatiotemporal resolution. Science 346, 1257998 (2014).
36. Mangeat, T. et al. Super-resolved live-cell imaging using random illumination microscopy. Cell Reports Methods 1, 100009 (2021).
37. Bigini, P. et al. The role and impact of polyethylene glycol on anaphylactic reactions to COVID-19 nano-vaccines. Nature Nanotechnology 16, 1169–1171 (2021).
38. Stewart, J.C. Colorimetric determination of phospholipids with ammonium ferrothiocyanate. Anal Biochem 104, 10–14 (1980).

Figures

Figure 1.

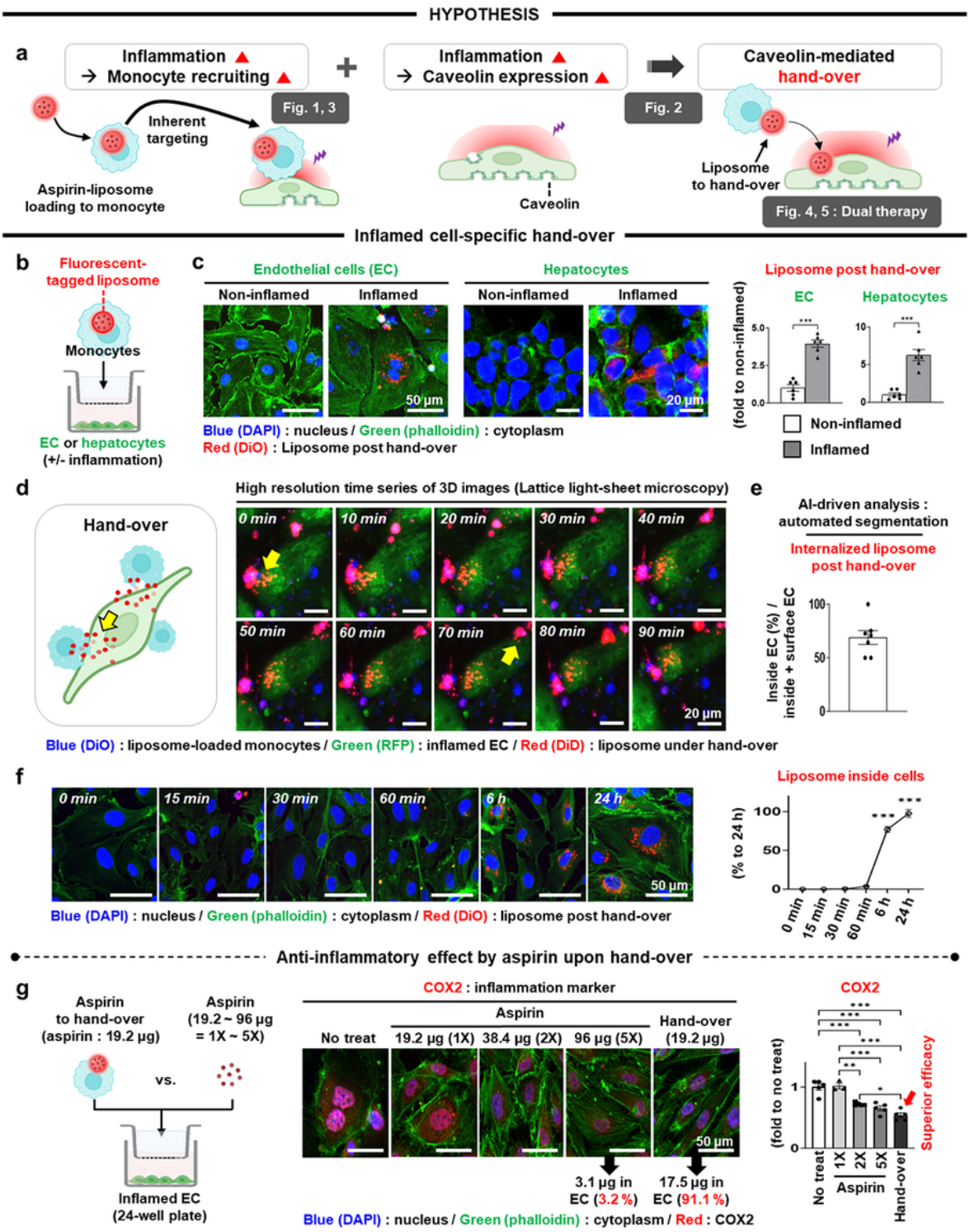

Figure 1

Liposomal loading to monocyte for hand-over to inflamed cells.

a. The hypothesis is that liposome loading to monocytes enables the subsequent hand-over to inflamed cells upon inherent targeting, which is dominantly mediated by caveolin as the expression is upregulated under inflammation. This strategy provides a foundation to approach the dual therapies which exerts the

aspirin effects to reduce i) not only the inflammation in target sites ii) but also platelet activation upon prolonged circulation. **b.** Fluorescent (DiO)-tagged liposomes are loaded into monocytes, which are then co-cultured with either ECs or hepatocytes in the top and bottom of trans-wells, respectively, as shown in the illustration. When inflammation is induced by LPS or ethanol, **c.** the inflamed ECs and hepatocytes (green phalloidin) uptake the liposome (red DiO) significantly more compared to non-inflamed condition as indicated by co-localization of red liposomes and green cytoskeleton. This result is confirmed by quantitative image analysis of internalized aspirin-liposome (N=6), thereby validating the inflamed cell-specific hand-over. **d.** It is possible for liposomes to attach merely on the membrane surface of inflamed cells rather than internalization. Hence, the 3D high-resolution imaging by lattice light-sheet microscopy captures the gradual internalization of liposomes (red DiD) into the inflamed ECs (green) through hand-over from the monocytes (blue DiO) over time. In the time series of images during 90 min on the single inflamed EC, the hand-over process from the monocytes is done by 60 min, and another monocyte starts the process around 70 min. **e.** The automated segmentation of AI-driven image analysis exhibits approximately 70 % internalization out of the total liposomes in the membrane and cytosol (N=7). **f.** Under the same imaging on inflamed ECs in a multi-time scale for 24 h, the significant increases of liposome internalization are visualized after 6 h, which continues afterward, as confirmed by quantitative image analysis (N=7 / p-value versus 0 min). **g.** The hand-over process is validated in another way by determining the anti-inflammatory effect of aspirin through the liposome internalization into inflamed ECs. After aspirin (19.2 μg) is encapsulated by liposomes, aspirin-liposomes are loaded into monocytes. The hand-over effect is compared with soluble treatment of aspirin by varying the concentration from 19.2 to 96 μg (1~5 fold : X) in the trans-well culture with inflamed ECs as shown in the illustration. As a result, the COX2 expression of ECs is suppressed significantly by the liposomal hand-over (19.2 μg). The same suppression effect is seen by increasing the soluble concentration up to 5X (96 μg, N=3-6), although the significant suppression starts at 2X soluble treatment. Of note, when the mass of internalized aspirin is determined by LC-MS analysis in this comparison, the hand-over enables 17.5 μg (91.1 %) of cellular uptake in contrast to 3.1 μg (3.2 %) of 5X soluble treatment. Endothelial cell (EC); lipopolysaccharide (LPS); red fluorescent protein (RFP); artificial intelligence (AI); cyclooxygenase 2 (COX2); liquid chromatography-mass spectrometry (LC-MS). Data = mean ± SEM (N: dots on each graph). *p < 0.05, **p < 0.01, and ***p < 0.001 between lined groups.

Figure 2.

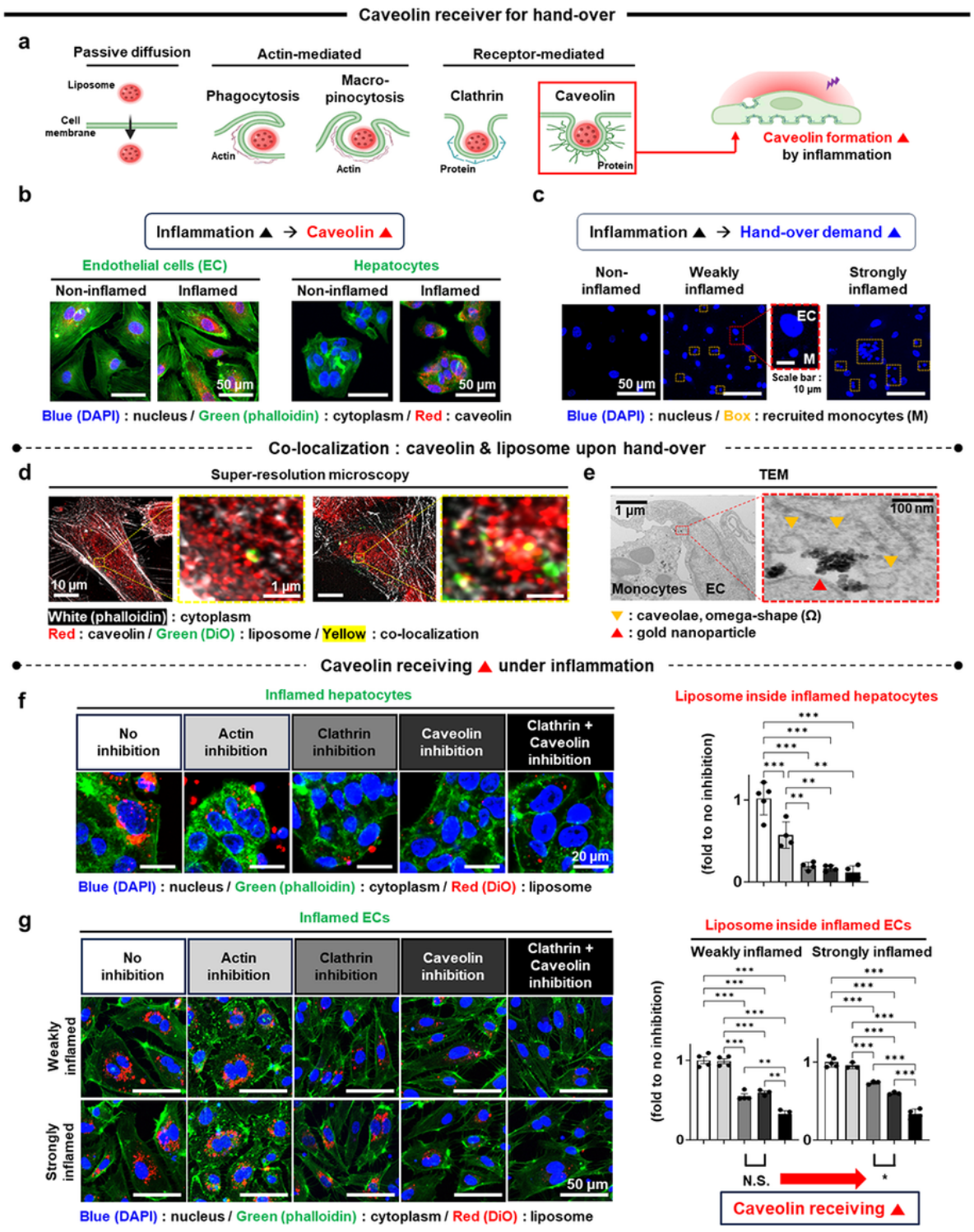

Figure 2

Caveolin as a key receiver of the hand-over through inflammatory upregulation of expression. a. Liposomes internalize into cells through i) passive diffusion, ii) actin-mediated penetration (phagocytosis and macro-pinocytosis), and iii) receptor-mediated process (clathrin and caveolin). Caveolin appears to play a key role in the hand-over process, which is processed by upregulation of caveolin expression under inflammation. **b.** Upon pro-inflammatory LPS treatment, both ECs and hepatocytes express caveolin (red)

visibly more compared to non-inflamed condition in the immunostaining images. **c.** As the degree of inflammation increases in the co-culture, more monocytes (yellow box : smaller nuclei) approach ECs (bigger nuclei), indicating increases in the demand of hand-over through upregulation of caveolin expression. **d.** Under imaging by super-resolution microscopy, the co-localization (yellow) between caveolin (red) and liposome (green) on ECs confirms the receiver role of caveolin in internalizing liposomes through the inflammatory hand-over. **e.**The co-localization between gold-liposome and caveolin (Ω shape) on the ECs confirms their integration under the hand-over from the adjacent monocytes. **f.** As another validation, the functions of actin, either clathrin or caveolin, and both are inhibited using cytochalasin D, active ingredient, active ingredient, and active ingredient-active ingredient, respectively, in the trans-well culture by adding red (DiO) fluorescent-tagged liposomes. The liposomal uptake by inflamed hepatocytes significantly decreases in all inhibition groups compared to no inhibition. The inhibition of actin function least decreases the liposomal uptake among the inhibition groups, and no clear differences are seen among the inhibition of receptor-mediated functions upon immunostaining with quantitative analysis (N=4-5). **g.** In the same setting with EC culture, the same results are seen except the significant decrease in the synergistic inhibition of both clathrin and caveolin compared to each inhibition. However, when the degree of inflammation is increased to a strong level, the receiver role of caveolin becomes more apparent as its inhibition significantly reduces the uptake compared to the inhibition of clathrin. The other comparison results remain in the same trends with those of weak inflammation (N=3-4). Lipopolysaccharide (LPS); endothelial cell (EC); transmission electron microscopy (TEM). Data = mean ± SEM (N: dots on each graph). *$p < 0.05$, **$p < 0.01$, and ***$p < 0.001$ between lined groups.

Figure 3.

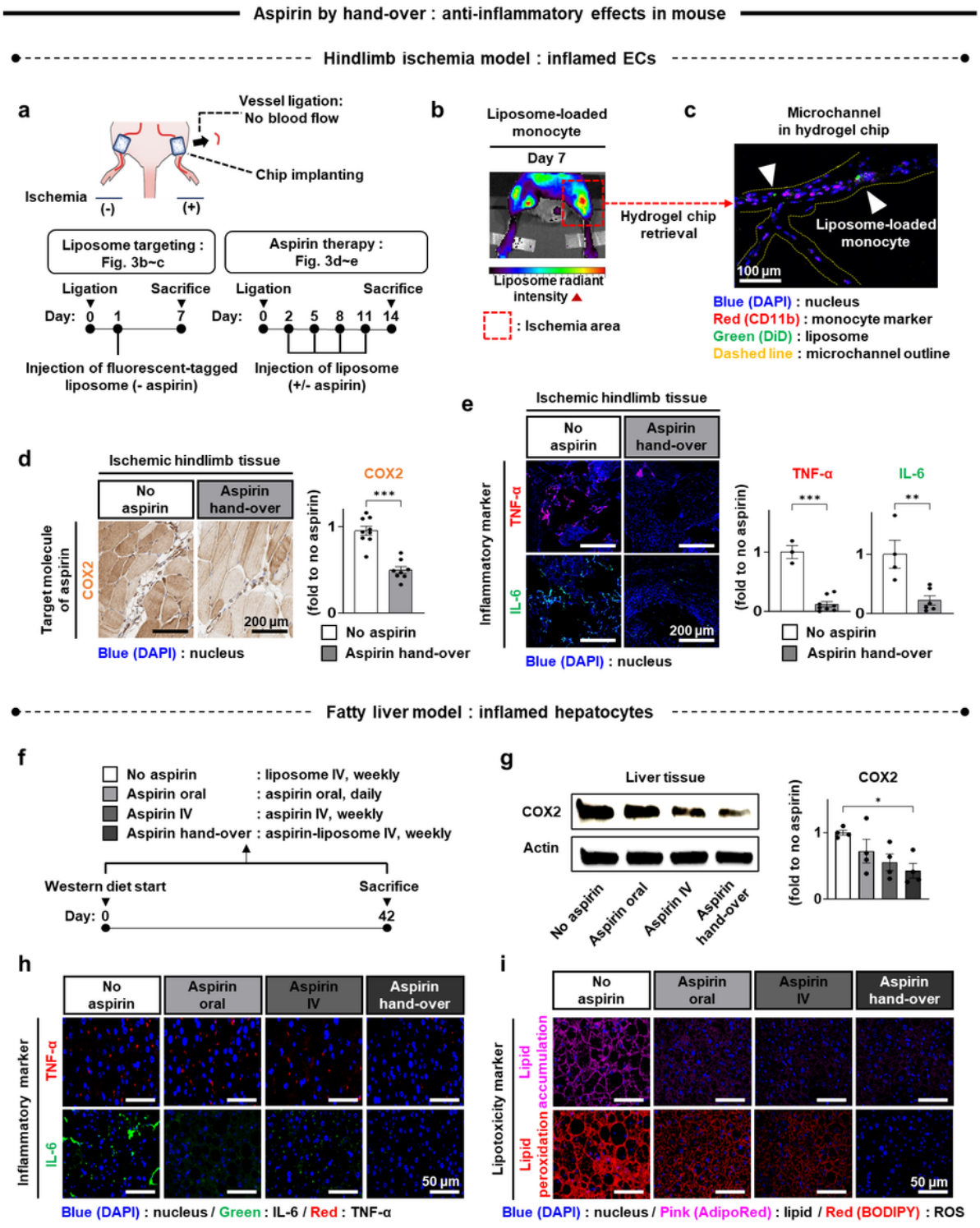

Figure 3

Anti-inflammatory effect of aspirin by hand-over to mouse inflamed sites. As one of the two mouse models to validate the hand-over process, **a.** the hindlimb ischemia model is used by implanting a microchannel hydrogel as a delivery bed upon blood reperfusion into inflamed ECs. First, liposomal targeting by monocyte carriers is examined by ligating the femoral artery with hydrogel implantation (Day 0), followed by tail vein injection of fluorescent-tagged liposomes (Day 1) and sacrifice (Day 7). Next, the

anti-inflammatory effect of aspirin through hand-over is determined by liposomal injection (+/- aspirin) every three-day (Day 2-11) post ligation, followed by sacrifice (Day 14). As a confirmation of targeting by liposome-loaded monocytes, **b.** IVIS imaging exhibits the elevated signal at the hydrogel of ischemic hindlimb compared to non-target sites in a radiant intensity range of $1–8 \times 10^7$. **c.** This result is further confirmed by harvesting the hydrogel with confocal imaging post immunostaining, which shows that monocytes (red CD11b) carry liposomes (green DiD) through microchannels (dashed line). As a validation of anti-inflammatory effect, **d.** the aspirin hand-over reduces COX2 expression in the ischemic hindlimb compared to no aspirin in immunostaining with quantitative analysis (N=8-9). **e.** This result is confirmed as other inflammatory markers such as TNF-α and IL-6 are significantly less expressed upon aspirin hand-over compared to no aspirin in immunostaining with quantitative analysis (N=3-8). **f.** As the other model, a fatty liver is generated by subjecting each apoE KO mouse to a western diet for 6 weeks. The weekly IV injection of liposome (+/- aspirin) or aspirin, and the daily oral injection of aspirin are compared in the therapeutic effect on inflamed hepatocytes. **g.** Compared to no aspirin, only the aspirin-liposome significantly reduces the COX2 expression in the fatty liver among the groups of aspirin injection in the western blot with quantitative analysis (N=4). This result is supported by the same trends in **h.** the expression of TNF-α and IL-6 as other markers of inflammation. **i.** The hand-over effect of aspirin-liposome is further evidenced in reducing lipid accumulation and peroxidation substantially as lipotoxicity markers. In vivo imaging system (IVIS); cyclooxygenase 2 (COX2); tumor necrosis factor-alpha (TNF-α); interleukin-6 (IL-6); apoE gene knockout (apoE KO); intravenous (IV); reactive oxygen species (ROS). Data = mean ± SEM (N: dots on each graph). *$p < 0.05$, **$p < 0.01$, and ***$p < 0.001$ between lined groups.

Figure 4.

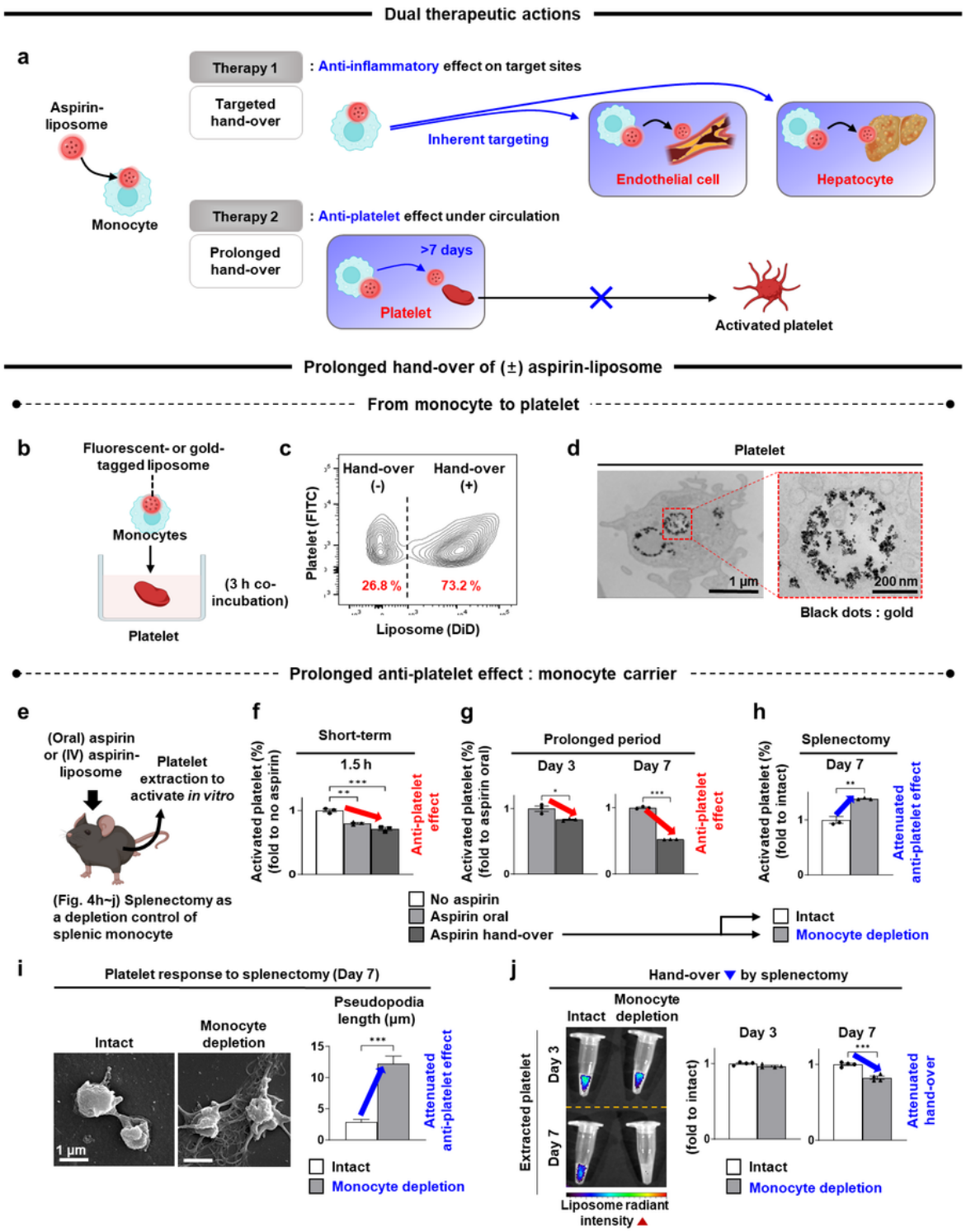

Figure 4

Prolonged hand-over to platelets under circulation as another dual therapeutic action. a. As the first action of dual therapies (Therapy 1), the anti-inflammatory therapy by hand-over has been shown so far through inherent targeting to inflamed ECs and hepatocytes by monocyte carriers of aspirin-liposome. As another dual action (Therapy 2), the prolonged anti-thrombosis therapy is approached by the hand-over of aspirin-liposome from monocytes to platelets under circulation over 7 days. **b.** DiD or gold-tagged

liposomes are loaded into monocytes, which are then incubated with platelets for 3 h in vitro. **c.** When fluorescent (DiD)-tagged liposomes are detected in FACS, 73.2 % platelets out of the total (100 %) in the culture uptake liposomes upon hand-over from monocytes. **d.** This result is confirmed by visualizing the circular localization of gold dots (10 nm, see the scale bar) under TEM as a presentation of liposomal uptake into a platelet. **e.** The in vivo action to suppress platelet activation is examined by tail vein injection of aspirin-liposome in comparison with oral injection of aspirin, followed by collecting blood and activating platelets in culture. Next, splenectomy is carried out as a depletion control of splenic monocytes so that the carrier role of monocytes in the hand-over to circulating platelets can be validated. **f.** Within a short -term (1.5 h) post injection in comparison with no aspirin, oral aspirin injection and aspirin hand-over significantly reduces the platelet activation in FACS analysis of CD62p expression as a representative marker of platelet activation (N=3). **g.** The same trend is seen from day 3 to 7 with significantly incremental reductions from oral aspirin injection to aspirin hand-over (N=3). **h.** The splenectomy significantly attenuates the anti-platelet effect compared to the intact hand-over at day 7 because the carrier function of splenic monocytes is absent (N=3). **i.** This result is confirmed by when platelets are isolated from these mice (Day 7) subjected to SEM imaging of platelet morphologies with quantitative analysis (N=34-37). The splenectomy results in the typical morphologies of activated platelets with rough surface and elongated pseudopodia as opposed to the morphologies of intact hand-over. **j.** Platelets are isolated from the mice post injection of fluorescent-tagged liposomes and subjected to IVIS analysis (N=4 / radiant intensity: 4.30-6.74 × 10^7). The effect of splenectomy is not seen on day 3 but becomes significant on day 7 in attenuating the anti-platelet effect, indicating the prolonged duration of therapeutic action. Fluorescence-activated cell sorting (FACS); transmission electron microscopy (TEM); intravenous (IV); scanning electron microscopy (SEM); in vivo imaging system (IVIS). Data = mean ± SEM (N: dots on each graph). *p < 0.05, **p < 0.01, and ***p < 0.001 between lined groups.

Figure 5.

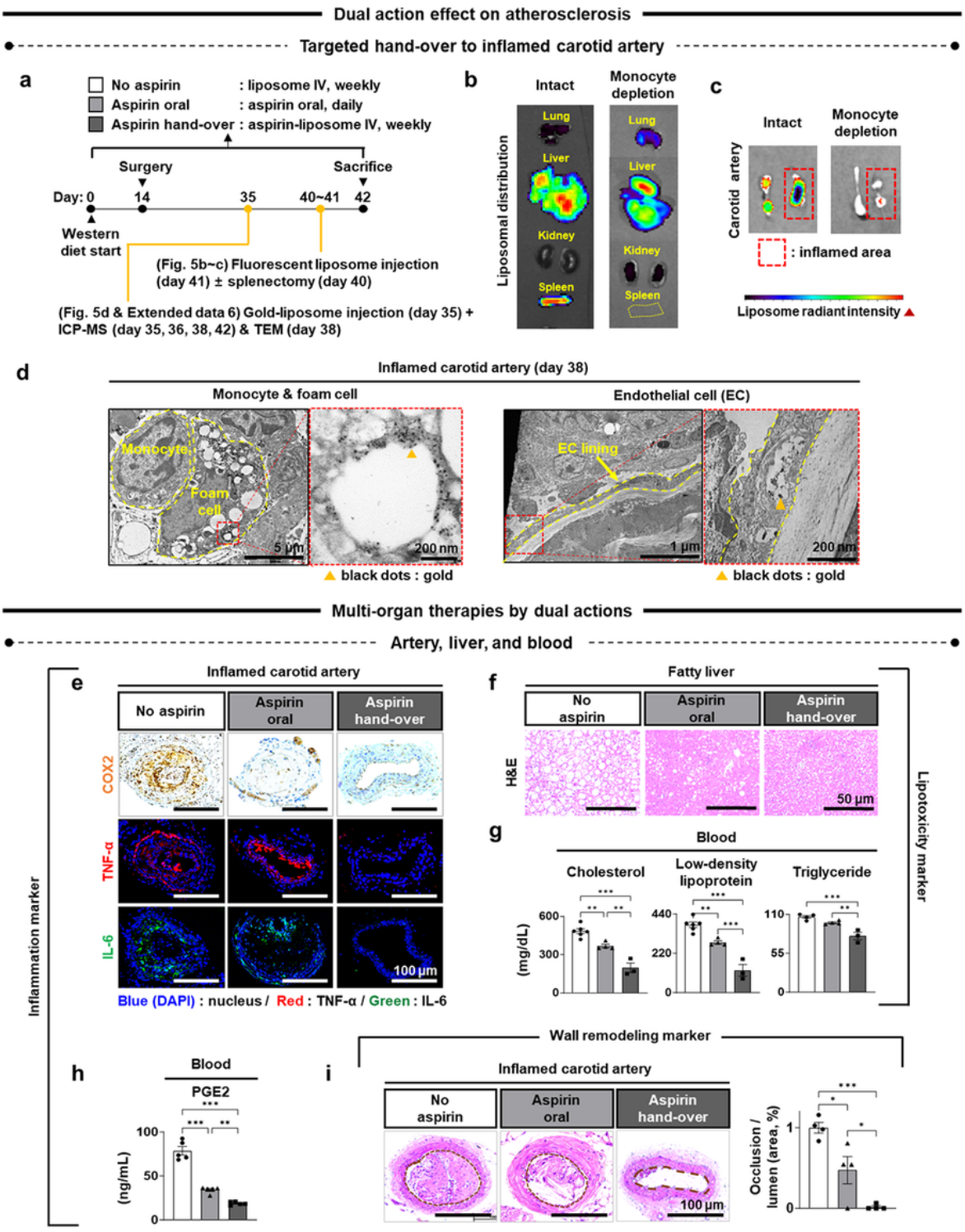

Figure 5

Targeted and multi-organ therapies by dual actions of hand-over on atherosclerosis. a. Atherosclerosis is induced in a carotid artery by subjecting apoE KO mice to western diet for 42 days with partial ligation of the artery by surgery on day 14. The weekly tail vein injection of liposomes (+/- aspirin) and the daily oral injection of aspirin are compared. **(b-c)** Splenectomy is conducted on day 40 with injection of fluorescent-tagged liposomes on day 41 with IVIS analysis (radiant intensity: 2.99-5.16 × 10^6). **(d & Extended data 6)**

Gold-tagged liposomes are injected on day 35 with analyses by ICP-MS (day 35, 36, 38, and 42) and TEM (day 38). **b.** The intact mice exhibit the majority of liposomal distribution into spleen and liver whereas the splenectomy mice show no splenic distribution with the strong and weak signals in liver and lung, respectively. **c.** The splenectomy results in nearly no targeting to the ligated carotid artery under inflammation in addition to the relatively weak signal in the non-ligated artery as well due to the depletion of splenic monocytes. In contrast, the intact mice exhibit more positive signals of liposomal distribution in the ligated artery compared to the non-ligated control. These results confirm the carrier role of splenic monocytes in the hand-over to the inflamed artery. **d.** Under TEM imaging, monocytes, foam cells (lipid-laden cells originated from monocytes), and ECs exhibit intracellular gold nanoparticles as evidence of targeted hand-over to the atherosclerotic artery. Next, due to the dual actions of hand-over therapy, **e.** the expression of inflammatory markers (COX2, TNF-α and IL-6) significantly decrease in the ligated carotid artery from no aspirin to oral aspirin injection and further to the aspirin hand-over by immunostaining. The same trends are confirmed in the liver **f.** with the reductions of lipid droplets by H&E staining and **g.** in the blood with the significant decreases of total cholesterol, low-density lipoprotein, and triglyceride levels **h.** as confirmed by the PGE2 levels which indicate blood inflammation (**g-h** : N=3-6). **i.** These multi-organ effects cooperate to suppress atherosclerosis of ligated carotid artery as the lesion formation significantly decreases from no aspirin to oral aspirin injection and further to the aspirin hand-over in quantitative H&E analysis (N=5). ApoE gene knockout (apoE KO); intravenous (IV); in vivo imaging system (IVIS); inductively coupled plasma-mass spectrometry (ICP-MS); transmission electron microscopy (TEM); endothelial cell (EC); cyclooxygenase 2 (COX2); tumor necrosis factor-alpha (TNF-α); interleukin-6 (IL-6); hematoxylin and eosin (H&E); prostaglandin E2 (PGE2). Data = mean ± SEM (N: dots on each graph). *p < 0.05, **p < 0.01, and ***p < 0.001 between lined groups.

Supplementary Files

This is a list of supplementary files associated with this preprint. Click to download.

- Extendeddata.docx